

Supplementary Material

Sustainable nitrogen-doped carbon electrodes for high-performance supercapacitors and Li-ion capacitors

Yulong Zheng,^a Huanlei Wang,^{*a} Shijiao Sun,^b Gaofei Lu,^a Haolin Liu,^a Minghua Huang,^a Jing Shi,^a Wei Liu,^a and Haiyan Li^{*a}

^a *School of Materials Science and Engineering, Ocean University of China, Qingdao 266100, PR China*

^b *College of Materials Science and Engineering, Nanjing Tech University, Nanjing 210009, PR China*

* Corresponding authors.

E-mail address: huanleiwang@ouc.edu.cn (H. Wang); lihy@ouc.edu.cn (H. Li)

Table S1. Relative surface concentrations (at.%) of nitrogen and oxygen moieties obtained by fitting the N 1s and O 1s core level XPS spectra

sample	N-6	N-5	N-Q	N-X	O-I	O-II	O-III
GSC	--	--	--	--	10.11	71.03	18.86
NGSC	29.1	14.8	34.81	21.3	16.05	55.14	28.81

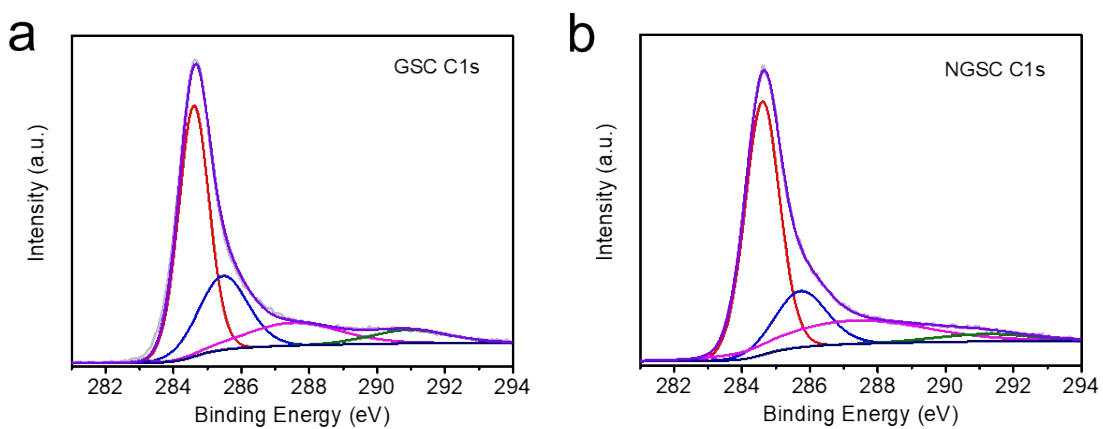


Figure S1. High-resolution XPS C1s spectra of (a) GSC and (b) NGSC samples.

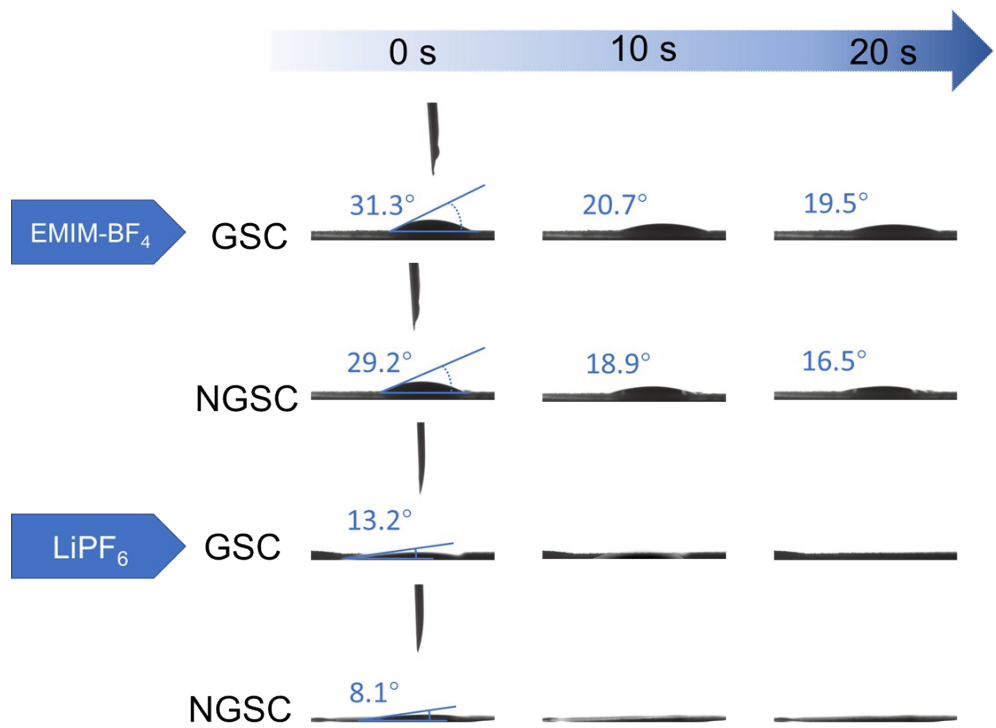


Figure S2. Dynamic contact angle measurement for the GSC and NGSC in EMIM-BF₄ and LiPF₆ electrolytes.

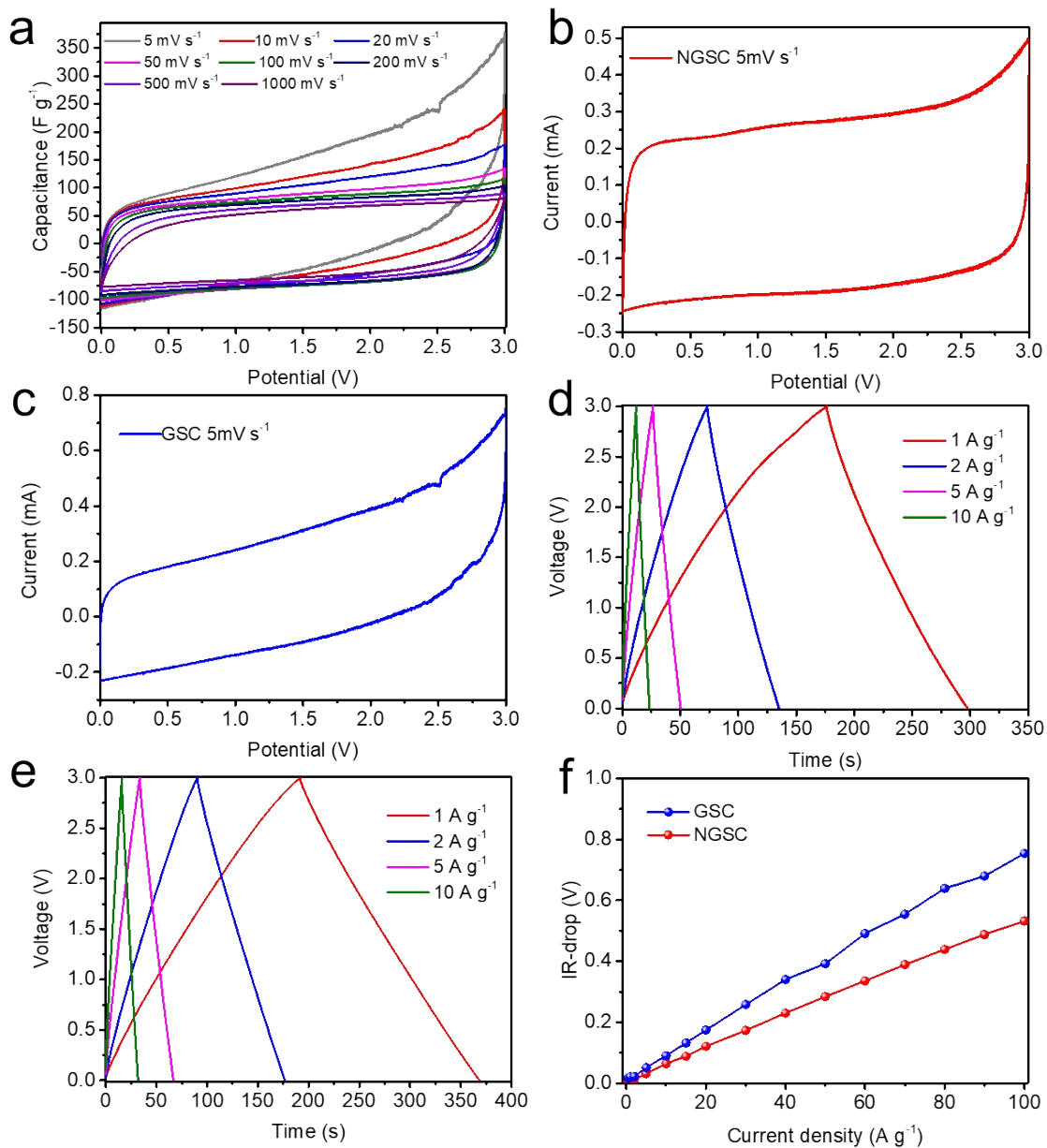


Figure S3. Electrochemical performance of ginger straw carbon as electrode for supercapacitors: (a) CV curves of GSC tested at various scan rates. CV curves of (b) NGSC and (c) GSC tested at 5 mV s^{-1} . Charge–discharge curves of (d) GSC and (f) NGSC at different current densities. (f) The IR-drop at different current densities.

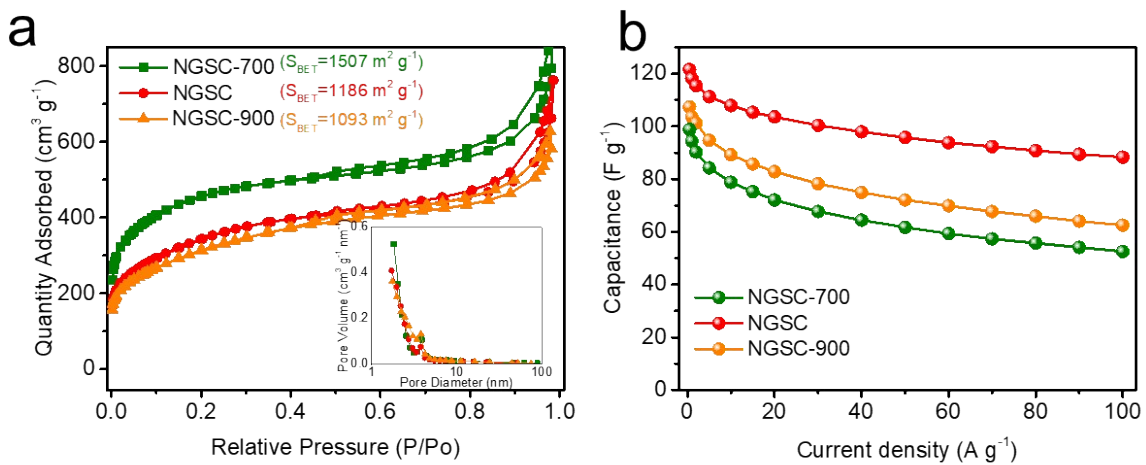


Figure S4. (a) The nitrogen adsorption-desorption isotherms of NGSC-700, NGSC and NGSC-900 and the inset is the related pore size distributions. (b) The specific capacitance as a function of current densities of NGSC-700, NGSC and NGSC-900 for ionic liquid-based supercapacitors.

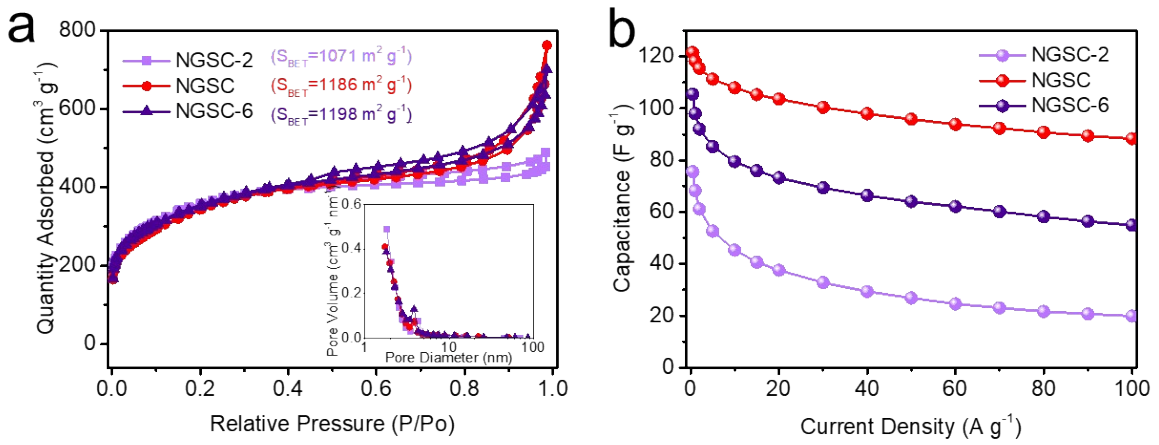


Figure S5. (a) The nitrogen adsorption-desorption isotherms of NGSC-2, NGSC and NGSC-6, and the inset is the related pore size distributions. (b) The specific capacitance as a function of current densities of NGSC-2, NGSC and NGSC-6 for ionic liquid-based supercapacitors.

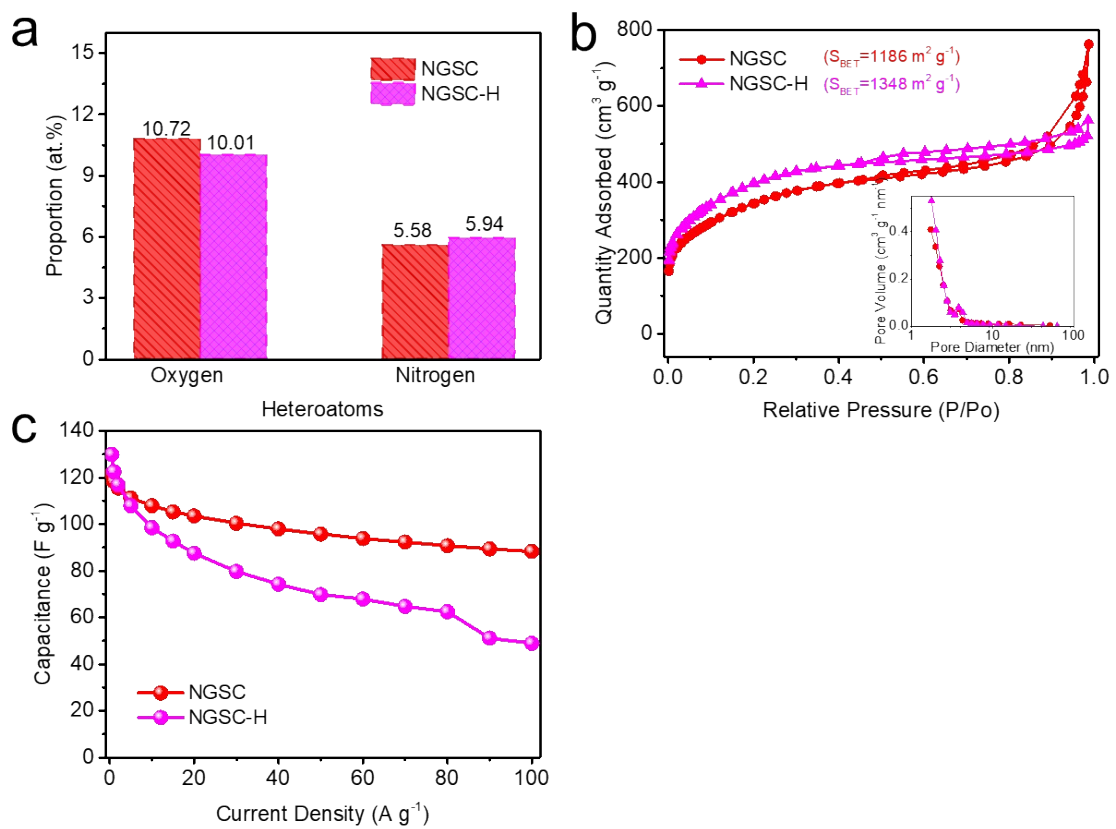


Figure S6. (a) Relative proportion of nitrogen and oxygen moieties on NGSC and NGSC-H. (b) The nitrogen adsorption-desorption isotherms of NGSC and NGSC-H, and the inset is their pore size distributions. (c) The specific capacitance as a function of current densities of NGSC and NGSC-H for ionic liquid-based supercapacitors.

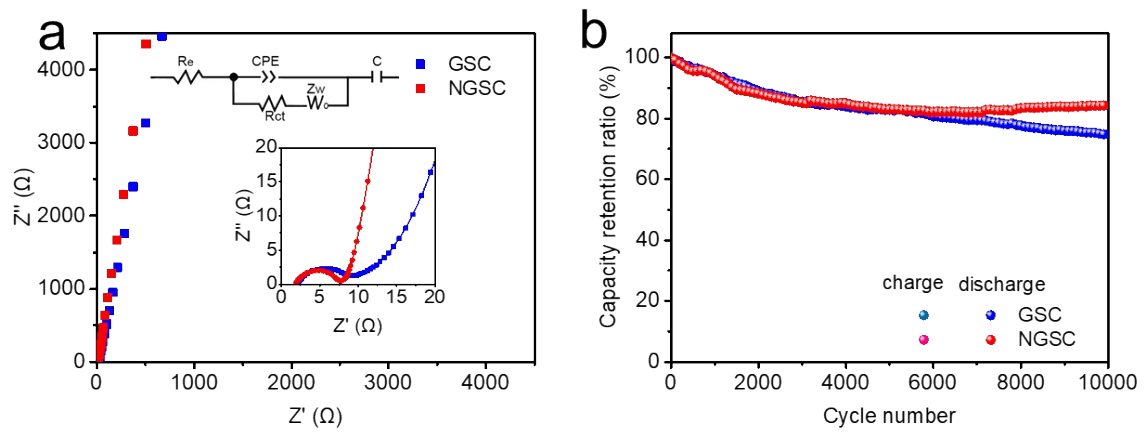


Figure S7. (a) Nyquist plots, and (b) the cycling performance at 10 A g^{-1} of GSC and NGSC electrodes.

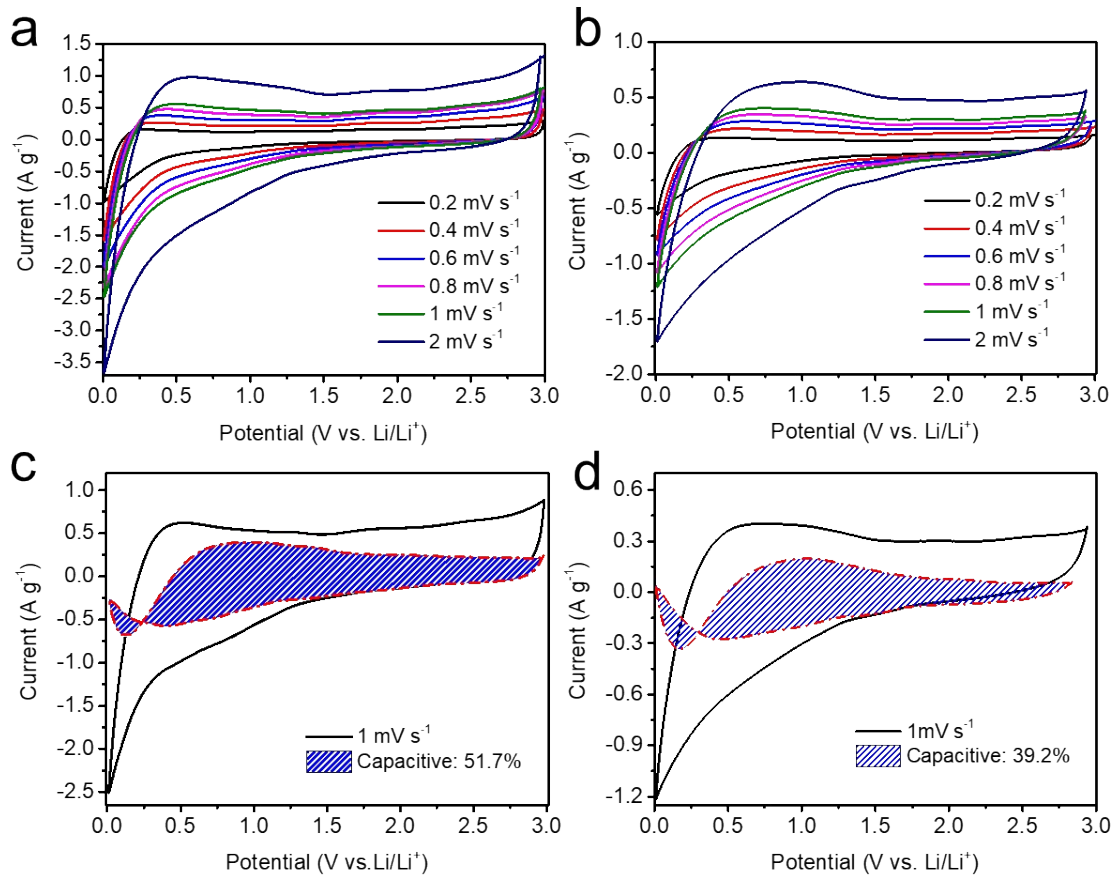


Figure S8. The electrochemical performance of ginger straw derived carbon as anode in half-cells: CV curves of (a) NGSC and (b) GSC tested at various scan rates. The capacitive contribution of (c) NGSC and (d) GSC at a scan rate of 1 mV s^{-1} .

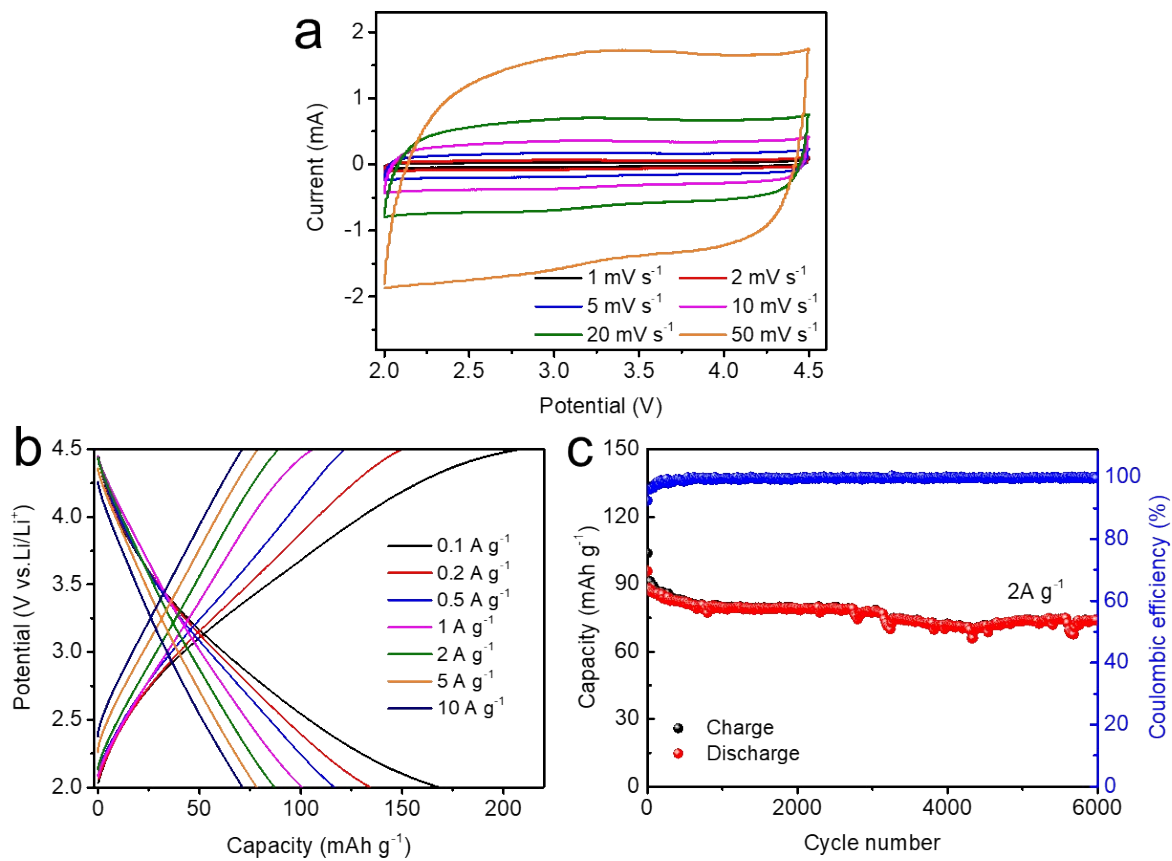


Figure S9. The electrochemical properties of NGSC as cathode in half-cells: (a) CV curves tested at different scan rates. (b) Galvanostatic charge-discharge curves at different current densities. (c) Cycling performance evaluated at 2 A g^{-1} .

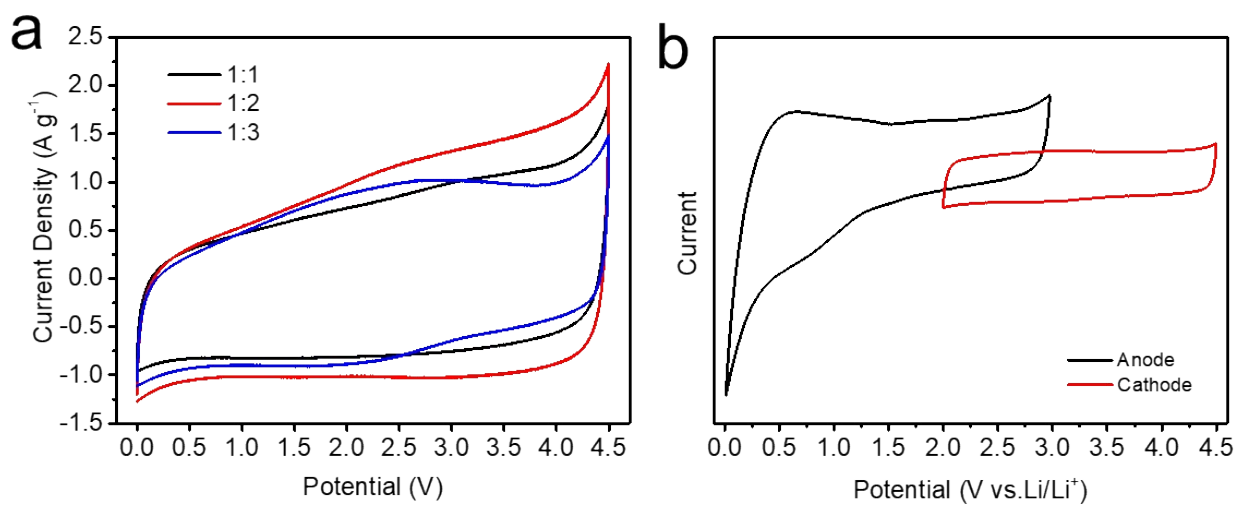


Figure S10. (a) Typical CV curves of lithium ion capacitors with different cathode to anode mass ratios measured at 20 mV s^{-1} . (b) Diagram of the operation potential range of anode and cathode for the NGSC//NGSC lithium ion capacitor configuration.

Table S2. Comparison of published electrochemical properties of Li-ion capacitors with this work

Hybrid System (anode//cathode)	Voltage window	Energy & Power	Capacity retention	Ref.
PHPNC//TiC	0-4.5	101.5 Wh kg ⁻¹ at 450 W kg ⁻¹ 23.4 Wh kg ⁻¹ at 67500 W kg ⁻¹	82% after 5000 cycles at 2 A g ⁻¹	1
ZMO-G//NCN	1-4	202.8 Wh kg ⁻¹ at 180 W kg ⁻¹ 98 Wh kg ⁻¹ at 21000 W kg ⁻¹	77.8% after 3000 cycles at 5 A g ⁻¹	2
MFC//3DaC	0-4	157 Wh kg ⁻¹ at 200 W kg ⁻¹ 58 Wh kg ⁻¹ at 20000 W kg ⁻¹	86.5% after 6000 cycles at 2 A g ⁻¹	3
MCMB//SFAC	2-4	83 Wh kg ⁻¹ at 128 W kg ⁻¹ 47 Wh kg ⁻¹ at 5718 W kg ⁻¹	92% after 1000 cycles at 0.5 A g ⁻¹	4
CTAB-Sn@Ti ₃ C ₂ /AC	1-4	105.5 Wh kg ⁻¹ at 495 W kg ⁻¹ 45.3 Wh kg ⁻¹ at 10800 W kg ⁻¹	71.1% after 4000 cycles at 2 A g ⁻¹	5
NOFC//PSNC	0-4	111 Wh kg ⁻¹ at 67 W kg ⁻¹ 38 Wh kg ⁻¹ at 14550 W kg ⁻¹	90% after 5000 cycles at 6.4 A g ⁻¹	6
Li ₃ VO ₄ //AC	1-4	136.4 Wh kg ⁻¹ at 532 W kg ⁻¹ 24.4 Wh kg ⁻¹ at 11020 W kg ⁻¹	87% after 1500 cycles at 2 A g ⁻¹	7
Si/C//AC	2-4.5	257 Wh kg ⁻¹ at 867 W kg ⁻¹ 147 Wh kg ⁻¹ at 29893 W kg ⁻¹	79.2% after 15000 cycles at 1.6 A g ⁻¹	8
SCN-A//SCN-A	0-4	112 Wh kg ⁻¹ at 67 W kg ⁻¹ 45 Wh kg ⁻¹ at 12000 W kg ⁻¹	82% after 3000 cycles at 5 A g ⁻¹	9
VO-CF//AC	2-4.3	112 Wh kg ⁻¹ at 23 W kg ⁻¹ 23.4 Wh kg ⁻¹ at ~8000 W kg ⁻¹	67% after 10000 cycles at 1.5 A g ⁻¹	10
BiVO ₄ //PRGO	0-4	152 Wh kg ⁻¹ at 384 W kg ⁻¹ 42 Wh kg ⁻¹ at 3861 W kg ⁻¹	81% after 6000 cycles at 0.9 A g ⁻¹	11
Ti ₃ C ₂ T _x /CNT//AC	1-4	67 Wh kg ⁻¹ at 258 W kg ⁻¹ 19 Wh kg ⁻¹ at 5797 W kg ⁻¹	81.3% after 5000 cycles at 2 A g ⁻¹	12

Si/Cu fabric//AC	1.5-4.2	210 Wh kg ⁻¹ at 193 W kg ⁻¹ 43 Wh kg ⁻¹ at 99000 W kg ⁻¹	90% after 30000 cycles at 10 A g ⁻¹	13
Co-CS//AC	2-4.3	108 Wh kg ⁻¹ at 200 W kg ⁻¹ 30 Wh kg ⁻¹ at ~8000 W kg ⁻¹	81% after 10000 cycles at 1.5 A g ⁻¹	14
Si/FG/C//CPAC	2-4.5	159 Wh kg ⁻¹ at 945 W kg ⁻¹ 99 Wh kg ⁻¹ at 31235 W kg ⁻¹	80% after 8000 cycles at 1 A g ⁻¹	15
SiG//AC	1-4	162 Wh kg ⁻¹ at 250 W kg ⁻¹ 60 Wh kg ⁻¹ at 11300 W kg ⁻¹	95% after 1300 cycles at 1 A g ⁻¹	16
NGSC// NGSC	0-4.5	214.6 Wh kg ⁻¹ at 373.5 W kg ⁻¹ 63.6 Wh kg ⁻¹ at 65400 W kg ⁻¹	82.7% after 10000 cycles at 50 A g ⁻¹	This work

References

1. H. Wang, Y. Zhang, H. Ang, Y. Zhang, H. T. Tan, Y. Zhang, Y. Guo, J. B. Franklin, X. L. Wu, M. Srinivasan, H. J. Fan and Q. Yan, *Adv. Funct. Mater.*, 2016, **26**, 3082-3093.
2. S. Li, J. Chen, M. Cui, G. Cai, J. Wang, P. Cui, X. Gong and P. S. Lee, *Small*, 2017, **13**, 1602893.
3. W. S. V. Lee, E. Peng, M. Li, X. Huang and J. M. Xue, *Nano Energy*, 2016, **27**, 202-212.
4. Z. Yang, H. Guo, X. Li, Z. Wang, Z. Yan and Y. Wang, *J. Power Sources*, 2016, **329**, 339-346.
5. J. Luo, W. Zhang, H. Yuan, C. Jin, L. Zhang, H. Huang, C. Liang, Y. Xia, J. Zhang, Y. Gan and X. Tao, *ACS Nano*, 2017, **11**, 2459-2469.
6. J. Ding, Z. Li, K. Cui, S. Boyer, D. Karpuzov and D. Mitlin, *Nano Energy*, 2016, **23**, 129-137.
7. L. Shen, H. Lv, S. Chen, P. Kopold, P. A. van Aken, X. Wu, J. Maier and Y. Yu, *Adv. Mater.*, 2017, **29**.
8. B. Li, F. Dai, Q. Xiao, L. Yang, J. Shen, C. Zhang and M. Cai, *Adv. Energy Mater.*, 2016, **6**, 1600802.
9. H. Wang, D. Mitlin, J. Ding, Z. Li and K. Cui, *J. Mater. Chem. A*, 2016, **4**, 5149-5158.
10. S. Jayaraman, G. Singh, S. Madhavi and V. Aravindan, *Carbon*, 2018, **134**, 9-14.
11. D. P. Dubal, K. Jayaramulu, R. Zboril, R. A. Fischer and P. Gomez-Romero, *J. Mater. Chem. A*, 2018, **6**, 6096-6106.
12. P. Yu, G. Cao, S. Yi, X. Zhang, C. Li, X. Sun, K. Wang and Y. Ma, *Nanoscale*, 2018, **10**, 5906-5913.
13. C.-M. Lai, T.-L. Kao and H.-Y. Tuan, *J. Power Sources*, 2018, **379**, 261-269.
14. S. Jayaraman, S. Madhavi and V. Aravindan, *J. Mater. Chem. A*, 2018, **6**, 3242-3248.

15. Q. Lu, B. Lu, M. Chen, X. Wang, T. Xing, M. Liu and X. Wang, *J. Power Sources*, 2018, **398**, 128-136.
16. C. Li, X. Zhang, K. Wang, X. Sun and Y. Ma, *J. Power Sources*, 2019, **414**, 293-301.